

## Communications to the Editor

### Phase Transitions and Honeycomb Morphology in an Incompatible Blend of Enantiomeric Polylactide Block Copolymers

Lu Sun,<sup>†</sup> Jorge E. Ginorio,<sup>†,§</sup> Lei Zhu,<sup>\*,†</sup> Igors Sics,<sup>‡</sup>  
Lixia Rong,<sup>‡</sup> and Benjamin S. Hsiao<sup>‡</sup>

*Polymer Program, Institute of Materials Science and Department of Chemical, Materials, and Biomolecular Engineering, University of Connecticut, Storrs, Connecticut 06269-3136, and Department of Chemistry, State University of New York at Stony Brook, Stony Brook, New York 11794-3400*

Received May 18, 2006

Revised Manuscript Received September 17, 2006

**Introduction.** Polylactide (PLA) is a biodegradable thermoplastic polymer, which can be obtained from renewable resources. The unique degradation properties of PLA have attracted a great deal of attention over the past few decades for a variety of biomedical, tissue engineering, and environmental applications.<sup>1,2</sup> Amphiphilic PLA block copolymers such as poly(ethylene oxide)–PLA (PEO–PLA) di- and triblock copolymers have been extensively studied due to their potential applications in the biomedical field, including injectable hydrogels for drug delivery,<sup>3</sup> tissue engineering,<sup>4</sup> and gene therapy,<sup>5</sup> just to name a few. Recently, hydrophobic PLA block copolymers have also attracted some attention. For example, PLA–poly( $\epsilon$ -caprolactone) (PCL) block copolymers has been demonstrated as biodegradable thermoplastic elastomers or shape memory polymers.<sup>6</sup> In nanotechnology, PLA block copolymers were used to fabricate nanoporous and monolith

polymeric materials,<sup>7,8</sup> where the facile degradability of PLA was utilized. All these applications make the fundamental understanding of the phase behaviors of PLA block copolymers a necessity.

Poly(L-lactide) (PLLA) and poly(D-lactide) (PDLA) are genuine enantiomeric chiral polymers. These enantiomeric polymers can crystallize into lamellar crystals with an orthorhombic unit cell with a melting temperature ( $T_m$ ) around 175 °C.<sup>9</sup> In 1987, Ikada et al. first reported the stereocomplex formation between enantiomeric PLLA and PDLA.<sup>10</sup> Compared to enantiomeric PLAs, PLA stereocomplexes exhibited a higher melting point (ca. 220–230 °C), higher mechanical strengths, and improved thermal and hydrolytic stability.<sup>11,12</sup> Stereocomplex formation in blends of compatible PLA block copolymers, such as PEO–PLA and PCL–PLA enantiomeric block copolymers, was also reported.<sup>13,14</sup> For example, novel biodegradable stereocomplex hydrogels for controlled drug delivery were developed based on PEO–PLA block copolymer stereocomplexes.<sup>15–17</sup> However, there have been only a few studies on the stereocomplex formation in incompatible PLLA and PDLA block copolymers. Kricheldorf et al. studied the stereocomplex formation and morphology in PLLA- and PDLA-containing A–B–A triblock copolymers with A being the PLA blocks.<sup>18</sup> By variation of the chemical structures of the B blocks using incompatible polymers, it was found that the attractive interactions between the PLLA and PDLA blocks, rather than the repulsive interactions between incompatible soft B blocks, dominated the stereocomplex formation and the final morphology.

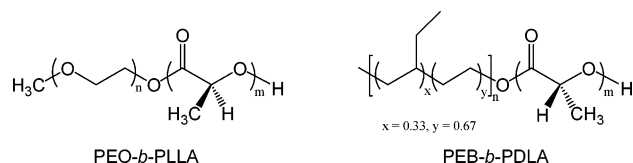
The morphology of the stereocomplexes comprised of incompatible enantiomeric PLA block copolymers in the melt has not yet been reported. In this report, two well-defined enantiomeric PLA block copolymers, poly(ethylene oxide)-*b*-PLLA (PEO-*b*-PLLA) and poly(ethylene-co-1-butene)-*b*-PDLA (PEB-*b*-PDLA), were successfully synthesized for this purpose. Quantitative stereocomplexes were obtained in an equimolar blend of PEO-*b*-PLLA and PEB-*b*-PDLA, where the PEO and PEB blocks were immiscible. Depending on different thermal treatments above the melting point of the stereocomplex, either

\* Corresponding author. E-mail: lei.zhu@uconn.edu. Telephone: 860-486-8708.

<sup>†</sup> Polymer Program, Institute of Materials Science and Department of Chemical, Materials, and Biomolecular Engineering, University of Connecticut.

<sup>‡</sup> Department of Chemistry, State University of New York at Stony Brook.

<sup>§</sup> Current address: Department of Chemical Engineering, University of Puerto Rico–Mayagüez, Mayagüez, Puerto Rico 00681.

**Scheme 1. Chemical Structures of PEO-*b*-PLLA and PEB-*b*-PDLA**

lamellar or inverted cylindrical morphology could be produced in the molten state at 205 °C. In particular, intriguing honeycomb morphology with the minor component PEB being the matrix was observed.

The two model diblock copolymers, PEO-*b*-PLLA and PEB-*b*-PDLA, were prepared (see Scheme 1) by controlled ring-opening polymerization of L- and D-lactides from PEO-OH (number-average molecular weight  $M_n = 2000$  g/mol and polydispersity index PDI = 1.07, purchased from Aldrich) and PEB-OH ( $M_n = 4200$  g/mol, 67% ethylene and 33% 1-butene, PDI = 1.06, purchased from Aldrich) in toluene, respectively, using 0.5 equiv of triethylaluminum ( $\text{AlEt}_3$ ) as the catalyst.<sup>19</sup> Synthesis and molecular characterization by size-exclusion chromatography (SEC) and proton nuclear magnetic resonance ( $^1\text{H}$  NMR) of PEO-*b*-PLLA and PEB-*b*-PDLA are described in the Supporting Information. From the  $^1\text{H}$  NMR analyses, the  $M_n$ s of the PLLA block in the PEO-*b*-PLLA and the PDLA block in the PEB-*b*-PDLA were both 5400 g/mol. The PDI for the PEO-*b*-PLLA and the PEB-*b*-PDLA were determined by SEC to be 1.12 and 1.09 (see Figure S2 in the Supporting Information), respectively. To prepare the stereocomplex, PEO-*b*-PLLA (2K–5.4K) and PEB-*b*-PDLA (4.2K–5.4K) were dissolved separately in chloroform at a concentration of ca. 10 wt %. Equimolar block copolymer blends were prepared by mixing the two solutions, followed by sufficient stirring, subsequent solvent evaporation in the hood, and drying in a vacuum oven at 50 °C for 3 d. The stereocomplex sample is denoted as SC5K–EO2K. Nearly 100% stereocomplex crystals, rather than the enantiomeric PLLA or PDLA crystals, were obtained after solution-casting. This was confirmed by the wide-angle X-ray diffraction (WAXD) results shown in Figure S4B in the Supporting Information.

To study the morphology in the melt (see Figure 1B, where all samples exhibited only an amorphous halo in the WAXD profiles), the SC5K–EO2K thin film cast from chloroform was heated to 250 °C, which was above the solution-cast stereocomplex melting temperature ( $T_m$ ) at 225 °C determined by differential scanning calorimetry (DSC). After the sample was isothermally held at 250 °C for 15 min (note that the PLA stereocomplexes exhibited much better thermal stability up to 260 °C than the enantiomers<sup>20</sup>), a relatively broad reflection with a  $d$ -spacing of 28.6 nm was seen in the small-angle X-ray scattering (SAXS) profile in Figure 1A-b. Judging from the position of its higher order reflection peak (weak and broad) at around  $0.43 \text{ nm}^{-1}$ , the morphology was expected to be a lamellar structure. Figure 2A shows the TEM micrograph of this lamellar structure with large undulations (note that a concentric lamellar structure is seen on the left). The bright lamellae were PEB layers and the dark microdomains were the mixed PEO and amorphous PLA phase. This is because PEB was resistant to  $\text{RuO}_4$  staining,<sup>21</sup> while amorphous PLA and PEO could be easily stained.<sup>22</sup> It is interesting to see that the PEB layer thickness appeared almost constant, no matter how the PEO/PLA layer thickness fluctuated.

When the SC5K–EO2K film was annealed at 250 °C for 1 min (see the SAXS profile in Figure 1A-a showing a  $d$ -spacing of 24.3 nm) and then quenched to 205 °C and held there for 60 min, a well-defined lamellar morphology with the  $q$ -ratio of peaks being 1:2 was observed in Figure 1A-c, where the overall  $d$ -spacing was 23.3 nm. Figure 2B shows the TEM micrograph of this lamellar structure, which possessed good uniformity in the lamellar thickness. Again, the PEB lamellae appeared bright, and its average thickness was about half of that of the dark PEO/PLA layers (see the inset in Figure 2B). This ratio is consistent with the volume fraction of the PEB in the blend (32 vol %).

If the SC5K–EO2K film was quenched to 205 °C and held there for 60 min after being first annealed at 250 °C for 15 min (see Figures 1A-b and 2A), a cylindrical morphology was observed with the  $q$ -ratio of peaks being  $1:\sqrt{3}:\sqrt{4}$  (see Figure 1A-d), despite a residue lamellar reflection at  $0.202 \text{ nm}^{-1}$  (31.1 nm, which is comparable with the long period of 28.6 nm in Figure

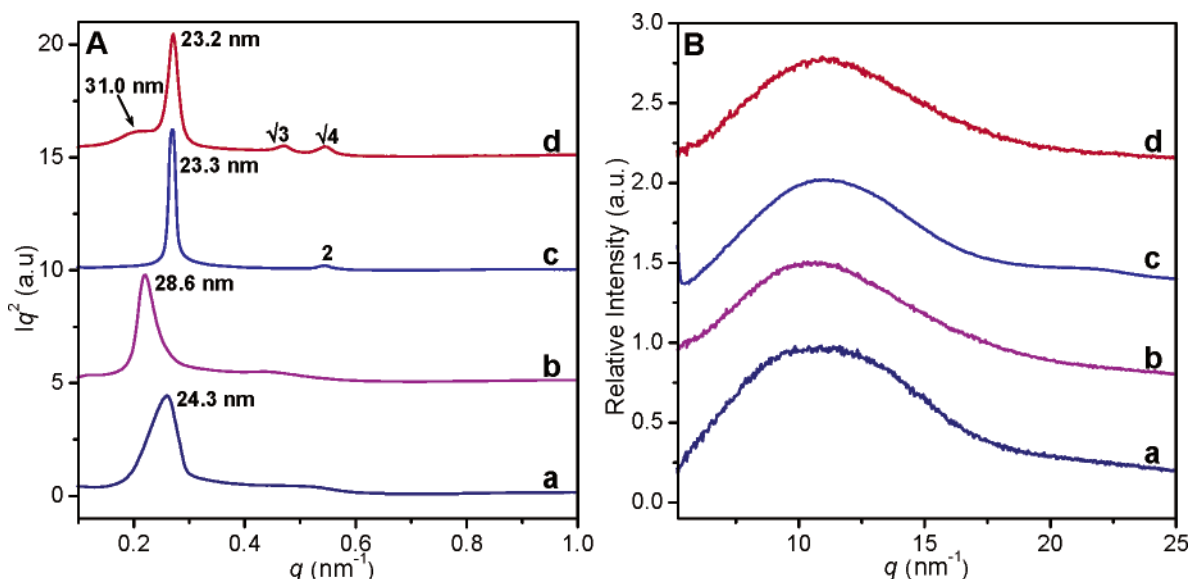


**Figure 1.** One-dimensional (A) SAXS and (B) WAXD profiles for the SC5K–EO2K with different thermal histories: (a) annealed at 250 °C for 1 min; (b) annealed at 250 °C for 15 min; (c) annealed at 205 °C for 60 min after holding at 250 °C for 1 min; (d) annealed at 205 °C for 60 min after holding at 250 °C for 15 min.

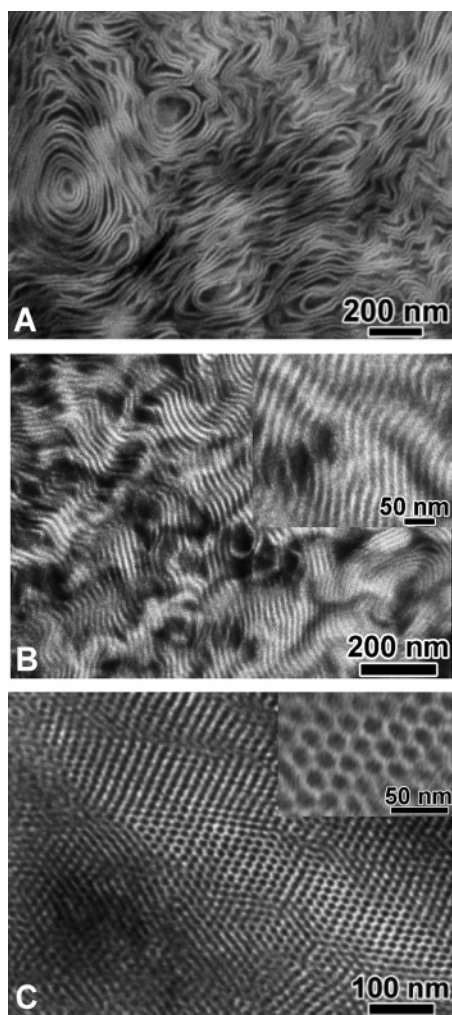


**Figure 2.** Bright-field TEM micrographs of the SC5K-EO2K samples deeply quenched to acetone/dry ice ( $-78\text{ }^{\circ}\text{C}$ ) after different thermal treatments in the melt: (A) SC5K-EO2K annealed at  $250\text{ }^{\circ}\text{C}$  for 15 min; (B) SC5K-EO2K annealed at  $205\text{ }^{\circ}\text{C}$  for 60 min after holding at  $250\text{ }^{\circ}\text{C}$  for 1 min; (C) SC5K-EO2K annealed at  $205\text{ }^{\circ}\text{C}$  for 60 min after holding at  $250\text{ }^{\circ}\text{C}$  15 min.

1A-b). Figure 2C shows the TEM micrograph of the cylindrical structure. Surprisingly, the minor component PEB did not form cylinders, as conventionally expected. Instead, it formed the matrix and the PEO/PLA components formed the cylinders. From the TEM micrograph (especially the inset of Figure 2C), the PEO/PLA cylinders exhibited a noncircular, hexagon-like shape, thus forming unique “honeycomb” morphology. Note that the hexagonal cross section of the cylinders could not be clearly seen possibly because of the diffuse boundaries between the bright and dark microdomains due to imperfect staining and/or stigmation of the TEM. Another TEM micrograph illustrating the honeycomb cylindrical morphology is shown in Figure S5 in the Supporting Information. Typical honeycomb morphology was reported in polystyrene-poly(2-vinylpyridine)-polybutadiene ABC heteroarm star terpolymers,<sup>23</sup> but not in diblock copolymers and their blends. Apparently, from both SAXS and TEM results, the SC5K-EO2K melt could have either lamellar or honeycomb morphology, depending on whether the sample was annealed at  $250\text{ }^{\circ}\text{C}$  for a short (1 min) or prolonged (15 min) time before quenching to  $205\text{ }^{\circ}\text{C}$  and being isothermally annealed for 60 min.

On the basis of the above results, tentative molecular models are proposed in Figure 3. It is seen that PLLA and PDLA formed 1:1 stereocomplexes after the blend was cast from chloroform.

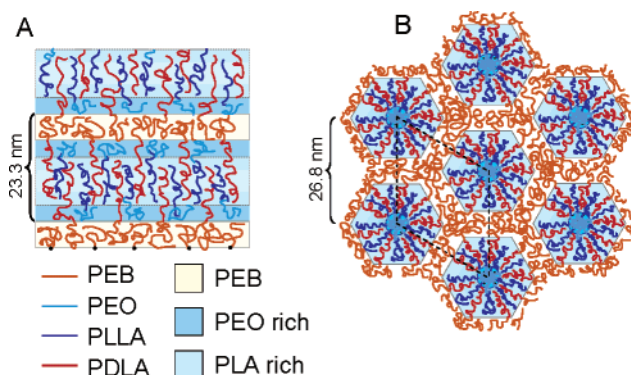


**Figure 3.** Schematic representations of (A) lamellar and (B) cylindrical (honeycomb) phases for the SC5K-EO2K samples after different thermal treatments.

The complexation process rejected the immiscible PEO and PEB blocks outside the lamellar crystals. Since chloroform is a good solvent for PEO and PEB blocks, PEO and PEB may form mixed brushes at both sides of a lamellar stereocomplex crystal during the crystallization from solution (see Figure S4, parts A and B, in the Supporting Information). When the sample was heated to  $250\text{ }^{\circ}\text{C}$  for a short time (e.g., 1 min), PLLA and PDLA did not have sufficient time to undergo large-scale reorganization and thus remained in the molten layers, even though the stereocomplex crystals had melted. Tsuji et al. proposed that in stereocomplexes the interaction between PLLA and PDLA were stronger than that between the chains with the same hand below  $260\text{ }^{\circ}\text{C}$ .<sup>24</sup> It may be the chiral interaction between PLLA and PDLA below  $260\text{ }^{\circ}\text{C}$  that induces PLLA/PDLA “pairing” in the melt. This “memory” effect of the stereocomplexes retained the lamellar morphology even when the blend was quenched to  $205\text{ }^{\circ}\text{C}$  and isothermally held there for 60 min. Because PEB is highly immiscible with PLA and PEO, the PEB microphase segregated from PLA and PEO microdomains. We know that amorphous PLA is compatible with amorphous PEO. However, it might be likely that the “memory” effect of PLLA/PDLA “pairing” in the melt induces PLA-rich and PEO-rich sublayers with a very diffuse boundary, as suggested in Figure 3A. This hypothesis, however, is subject to further investigation.

After being annealed at  $250\text{ }^{\circ}\text{C}$  for a sufficient time (e.g., 15 min), the molecules and microdomains began to reorganize. Since PEB occupied only 32 vol %, the equilibrium morphology such as PEB cylinders should be favored. Surprisingly, instead of the minor component PEB forming the cylinders, it formed the matrix. A schematic model is shown in Figure 3B. Assuming the hydrocarbon PEB was more immiscible with hydrophilic PEO than with hydrophobic PLA, contact between the PEB and PEO was minimized as the system reorganized toward the equilibrium. As a result, PEB blocks had to flip to one side and PEO to the other side of a PLA-rich microdomain (possibly due to the “memory” effect) to reduce contacts between PEB and PEO. This is different from the schematic representation in Figure 3A, where two PEO-rich layers are in direct contact with a PEB layer. Because of the difference in the molecular weights of PEB-4.2K and PEO-2K blocks, unbalanced surface tensions at both sides of a PLA-rich layer would force it to bend into a cylinder with a PEO-2K rich microdomain at the center and PEB at the periphery of the cylinders, as shown in Figure 3B. However, it is still unclear why the PLA/PEO cylinders exhibited a non-circular hexagonal shape as observed experimentally. Further investigation is necessary to answer this question. The large-scale reorganization of PEB and PEO



flipping to the opposite sides of a PLA-rich layer is consistent with the TEM observation in Figure 2A.

In conclusion, using SAXS and TEM techniques, we have observed thermal history-dependent mesophase transitions in an incompatible blend of enantiomeric PLA block copolymers, PEO-*b*-PLLA (2K–5.4K) and PEB-*b*-PDLA (4.2K–5.4K). Annealing at 250 °C for a short time (1 min) resulted in lamellar morphology, while annealing at 250 °C for a longer time (15 min) resulted in inverted honeycomb morphology. These morphologies can be tentatively explained by the “memory” effect that PLLA and PDLA still had complementary chiral interactions and thus formed a PLA-rich molten microdomain, even though their stereocomplex crystals were completely melted at 250 °C. The two morphologies in the melt were kinetics dependent; the lamellar morphology was kinetically favored while the honeycomb morphology was thermodynamically favored.

As a comparison, an equimolar PEO-*b*-PLLA (2K–5.4K) and PEB-*b*-PLLA (4.2K–5.4K) blend was also studied in the melt (data not shown). Preliminary TEM results showed macrophase separation instead of microphase separation in the blend. This indirectly proved that the complementary chiral interaction between PLLA and PDLA played an important role in reaching the final morphology in the molten SC5K–EO2K blend.

**Acknowledgment.** This work was supported by the donors of the Petroleum Research Fund, administered by the American Chemical Society, Grant ACS PRF 41918-G7, and NSF CAREER award DMR-0348724. J.E.G. thanks the NSF REU program (DMR-0353894). The synchrotron X-ray experiments were carried out at the National Synchrotron Light Source in Brookhaven National Laboratory, supported by the U.S. Department of Energy.

**Supporting Information Available:** Text giving the experimental details for this paper and figures showing <sup>1</sup>H NMR spectra of PEB-*b*-PDLA (4.2K–5.4K) and PEO-*b*-PLLA (2K–5.4K) diblock copolymers, SEC curves for PEB-*b*-PDLA (4.2K–5.4K), PEO-*b*-PLLA (2K–5.4K), PEB-4.2K, and PEO-2K, transmission electron microscopy (TEM) micrograph of a PEB-*b*-PDLA (4.2K–10.7K) diblock copolymer, 1D Lorentz-corrected SAXS profile for SC5K–EO2K cast from chloroform and WAXD profiles of PEB-*b*-PDLA (4.2K–5.4K), PEO-*b*-PLLA (2.0K–5.4K), and SC5K–EO2K, cast from chloroform at room temperature, and a sample

bright-field TEM micrograph of the stereocomplex SC5K–EO2K sample. This material is available free of charge via the Internet at <http://pubs.acs.org>.

## References and Notes

- (1) Uhrich, K. E.; Cannizzaro, S. M.; Langer, R. S.; Shakesheff, K. M. *Chem. Rev.* **1999**, *99*, 3181–3198.
- (2) Kricheldorf, H. *Chemosphere* **2001**, *43*, 49–54.
- (3) Jeong, B.; Bae, Y. H.; Lee, D. S.; Kim, S. W. *Nature (London)* **1997**, *388*, 860–862.
- (4) Lee, S.-H.; Kim, B.-S.; Kim, S. H.; Kang, S. W.; Kim, Y. H. *Macromol. Biosci.* **2004**, *4*, 802–810.
- (5) Luu, Y. K.; Kim, K.; Hsiao, B. S.; Chu, B.; Hadjiargyrou, M. *J. Controlled Release* **2003**, *89*, 341–353.
- (6) Cohn, D.; Hotovely-Salomon, A. *Biomaterials* **2005**, *26*, 2297–2305.
- (7) Zalusky, A. S.; Olayo-Valles, R.; Wolf, J. H.; Hillmyer, M. A. *J. Am. Chem. Soc.* **2002**, *124*, 12761–12773.
- (8) Rzaev, J.; Hillmyer, M. A. *Macromolecules* **2005**, *38*, 3–5.
- (9) Cartier, L.; Okihara, T.; Ikada, Y.; Tsuji, H.; Puiggali, J.; Lotz, B. *Polymer* **2000**, *41*, 8909–8919.
- (10) Ikada, Y.; Jamshidi, K.; Tsuji, H.; Hyon, S. H. *Macromolecules* **1987**, *20*, 904–906.
- (11) Tsuji, H. *Macromol. Biosci.* **2005**, *5*, 569–597.
- (12) Slager, J.; Domb, A. J. *Adv. Drug Delivery Rev.* **2003**, *55*, 549–583.
- (13) Stevels, W. M.; Ankone, M. J. K.; Dijkstra, P. J.; Feijen, J. *Macromol. Chem. Phys.* **1995**, *196*, 3687–3694.
- (14) Stevels, W. M.; Ankone, M. J. K.; Dijkstra, P. J.; Feijen, J. *Macromol. Symp.* **1996**, *102*, 107–113.
- (15) Grijpma, D. W.; Feijen, J. *J. Controlled Release* **2001**, *72*, 247–249.
- (16) Kissel, T.; Li, Y. X.; Unger, F. *Adv. Drug Delivery Rev.* **2002**, *54*, 99–134.
- (17) Hiemstra, C.; Zhong, Z. Y.; Dijkstra, P.; Feijen, J. *Macromol. Symp.* **2005**, *224*, 119–131.
- (18) Kricheldorf, H. R.; Rost, S.; Wutz, C.; Domb, A. *Macromolecules* **2005**, *38*, 7018–7025.
- (19) Schmidt, S. C.; Hillmyer, M. A. *Macromolecules* **1999**, *32*, 4794–4801.
- (20) Tsuji, H.; Fukui, I. *Polymer* **2003**, *44*, 2891–2896.
- (21) Kim, J. K.; Lee, H. H.; Sakurai, S.; Aida, S.; Masamoto, J.; Nomura, S.; Kitagawa, Y.; Suda, Y. *Macromolecules* **1999**, *32*, 6707–6717.
- (22) For PEO staining by RuO<sub>4</sub>, see: Sun, L.; Liu, Y.; Zhu, L.; Hsiao, B. S.; Avila-Orta, C. A. *Macromol. Rapid Commun.* **2004**, *25*, 853–857. For PLA staining by RuO<sub>4</sub>, see Figure S3 in the Supporting Information; the amorphous PDLA-10.7K lamellae appeared dark, while the PEB-4.2K layers were bright after RuO<sub>4</sub> staining.
- (23) Hückstädt, H.; Göpfert, A.; Abetz, V. *Macromol. Chem. Phys.* **2000**, *201*, 296–307.
- (24) Tsuji, H.; Fukui, I. *Polymer* **2003**, *44*, 2891–2896.

MA061115B